UPPSALA
UNIVERSITET

Digital Comprehensive Summaries of Uppsala Dissertations from the Faculty of Science and Technology 575

Mineral Reactions and Slag Formation During Reduction of Olivine Blast Furnace Pellets

ELIN RYÖSÄ

ACTA
UNIVERSITATIS
UPSALIENSIS
UPPSALA
2008

ISSN 1651-6214
ISBN 978-91-554-7340-2
urn:nbn:se:uu:diva-9389

Dissertation presented at Uppsala University to be publicly examined in Axel Hambergsalen, Geocentrum, Villavägen 16, 752 36 Uppsala, Thursday, November 20, 2008 at 10:00 for the degree of Doctor of Philosophy. The examination will be conducted in English.

Abstract
Ryösä, E. 2008. Mineral Reactions and Slag Formation During Reduction of Olivine Blast Furnace Pellets. Acta Universitatis Upsaliensis. *Digital Comprehensive Summaries of Uppsala Dissertations from the Faculty of Science and Technology* 575. 45 pp. Uppsala. ISBN 978-91-554-7340-2.

The present work focuses on mineral reactions and slag formation of LKAB olivine iron ore pellets (MPBO) subjected to reducing conditions in the LKAB experimental blast furnace (EBF). The emphasis is on olivine reactions with surrounding iron oxides. Many factors influence the olivine behaviour. The study was performed by use of micro methods; optical microscopy, micro probe analysis, micro Raman and Mössbuer spectroscopy and thremodynamic modeling. During manufacturing, in oxidising atmosphere at high temperature (1350°C), olivine alterations occur through slag formation and rim reactions with iron oxides and other additives. To be able to describe olivine behaviour in the rather complex blast furnace reduction process one has to consider factors such as reactions kinetics, reduction degree of iron oxides, vertical and horizontal position in the furnace and reactions with alkali. Samples were collected from the EBF both from in shaft probing during operation and from excavation following quenching of the EBF.

The initial slag forming olivine consist of primary forsterite – (Mg1.9Fe0.1)SiO4 – with inclusions of hematite and an amorphous silica rich phase, a first corona with lamellae of magnesioferrite, olivine and orthopyroxene, a second corona of amorphous silica and magnesioferrite. During reduction in the upper shaft in the EBF (700-900°C) Fe3+ reduces to Fe2+. The amorphous silica in the second corona absorbs alkali, Al, Fe2+, Mg, and Ca and form glasses of varying compositions. The lamellae in the first corona will merge into a single phase olivine rim. With further reduction the glasses in the second corona will merge with the olivine rim forming an iron rich olivine rim and leaving the elements that do not fit into the olivine crystal lattice as small silicate glass inclusions. Diffusion of magnesium and iron between olivines and iron oxides increase with increasing temperature in the lower shaft of the EBF (750-1100°C). In the cohesive zone of the EBF (1100-1200°C) Fe2+ is not stable any longer and Fe2+ will be expelled from the olivine as metallic iron blebs, and the olivine will form a complex melt with a typical composition of alkali-Al2O3-MgO-SiO2. Alkali plays an important role in this final olivine consumption.

The quench time for samples collected with probes and excavation are minutes respectively hours. A study of the quench rate's effect on the phases showed no differences in the upper shaft. However, in the lower shaft wüstite separates into wüstite and magnetite when wüstite grows out of its stability field during slow cooling of excavated samples. There is also a higher alkali and aluminium deposition in the glass phases surrounding olivines in excavated pellets as a result of alkali and aluminium gas condensing on the burden in the EBF during cooling.

Coating applied to olivine pellets was studied in the EBF with the aim to investigate its behaviour, particularly its ability to capture alkali. The coating materials were kaolinite, bauxite, olivine and limestone. No significant reactions were observed in the upper shaft. In the lower shaft a majority of the phases were amorphous and reflecting the original coating compositions. Deposition from the EBF gas phase occurs and kalsilite (KAlSiO4) is found in all samples; coating used for binding alkali is redundant from a quality perspective.

Keywords: olivine, iron ore pellets, blast furnace, reduction, alkali, coating, slag formation

Elin Ryösä, Department of Earth Sciences, Villav. 16, Uppsala University, SE-75236 Uppsala, Sweden

ISSN 1651-6214

ISBN 978-91-554-7340-2
urn:nbn:se:uu:diva-9389 (http://urn.kb.se/resolve?urn=urn:nbn:se:uu:diva-9389)

List of Papers

This thesis is based on the following papers, which are referred to in the text by their Roman numerals.

I Eliasson, E., Hooey, P.L., Annersten, H., and Lindblom, B. (2007) Formation of Potassium Slag in Olivine Fluxed Blast Furnace Pellets. *Ironmaking and Steelmaking*, 34, 5:422-430

II Ryösä, E., Wikström, J., Lindblom, B., Rutqvist, E., Benedictus, A., and Butcher, A. (2008) Investigation of Minerals and Iron Oxide Alterations in Olivine Pellets Excavated from the LKAB Experimental Blast Furnace. *Proceedings – Ninth International Congress for Applied Mineralogy*: 545-555

III Ryösä, E., Annersten, H., Rutqvist, E., and Lindblom, B. (2008) Behaviour of Coatings on Olivine Fluxed Pellets in Blast Furnace Reduction. *Steel Research International*, **accepted.**

IV Ryösä, E., Lindblom, B., and Annersten, H. (2008) Effect of Quench Rate on Phases in Olivine Fluxed Blast Furnace Pellets, **Manuscript.**

V Ryösä, E. (2008) Olivine Reactions during Reduction in Blast Furnace Pellets, **Manuscript.**

VI Annersten, H., and Ryösä, E. (2008) Monitoring Reduction Degree of Olivine Fluxed Blast Furnace Pellets from Mössbauer Spectra, **Manuscript.**

When Ryösä is first author she has been the main author and conducted the scientific work with helpful discussions from the co-authors. Annersten was the main author of Paper VI with valuable contributions from Ryösä.

Contents

1. Introduction 7
1.1 Aims of Study 8
1.2 Olivine Mineral 8
1.3 Mineral Reactions in the Pelletising Process 8
1.4 Alkali Cycle in the Blast Furnace 9
1.5 Effects of Quench Time on Pellets 9
1.6 Effects of Coating on Pellets 9

2. Methodology 11

3. Olivines in oxidised pellets 16

4. Olivines in reduced pellets 18
4.1 Upper Shaft of the Experimental Blast Furnace 18
4.2 Lower Shaft of the Experimental Blast Furnace 21
4.3 Cohesive Zone of the Experimental Blast Furnace 23
4.4 Magnesium and Iron Reactions between Olivine, Glass and Iron Oxides 25

5. Quantitative study of olivine and slag in reduced pellets 26

6. Kinetics in reduced pellets 30

7. Coating 32
7.1 Upper Shaft of the Experimental Blast Furnace 32
7.2 Lower Shaft of the Experimental Blast Furnace 33

8. Reduction of Iron Oxides Monitored with Mössbauer Spectroscopy 34

9. Summary of the Papers 35
9.1 Formation of Potassium Slag in Olivine Fluxed Blast Furnace Pellets 35
9.2 Investigation of Minerals and Iron Oxide Alterations in Olivine Pellets Excavated from LKAB Experimental Blast Furnace 35
9.3 Behaviour of Coatings on Olivine Fluxed Pellets in Blast Furnace Reduction 36

9.4 Effect of Quench Rate on Phases in Olivine Fluxed Blast Furnace Pellets 36
9.5 Olivine Reactions During Reduction in Blast Furnace Pellets 37
9.6 Monitoring Reduction Degree of Olivine Fluxed Blast Furnace Pellets from Mössbauer Spectra 37

10. Concluding Remarks 39

11. Summary in Swedish 41
Mineralreaktioner och slaggbildning under reduktion av masugnspellets med olivintillsats 41

Acknowledgements 43

References 44

1. Introduction

Iron ore pellets are commonly used in the modern blast furnace process. The pellets are made by adding binder to finely ground iron ore and pelletised in a balling drum or disc pelletiser. These so called *green pellets* are fired in an induration process up to 1350°C. Several additives may be added to gain certain slag forming properties in the blast furnace.

Important characteristics of pellets in the blast furnace are their reducibility, low temperature disintegration, strength after reduction, swelling and softening. Softening at low temperatures lead to closure of pores and decrease in permeability. It is thus desirable to have high softening and melting temperatures. Further it is desirable to have a short temperature interval between softening and melting to allow maximum gas permeability.

The use of magnesium in pellets makes the softening and melting zone in the blast furnace narrower (Narita, 1978 and Brämming and Wikström, 2002). Other beneficial qualities with the use of magnesium are; higher productivity, lower coke rate and better desulphurisation. After partial reduction at 900°C the strength of pellets is increased with the addition of magnesium to pellets by raising the melting point of slag phases. Less amount of liquid slag early in the blast furnace gives higher porosity which promotes the reducibility of the iron oxides.

LKAB use olivine with forsteritic composition today as a magnesium source in their pellets. Further additives to LKAB's blast furnace pellets are quartz and limestone. Quartz reacts with the iron oxides and forms a relatively low melting slag phase of fayalitic composition (Lu et al, 1985). The limestone is completely decomposed in the pelletising process (Niiniskorpi, 2004). Calciumferrites form which increase the strength of pellets in the low temperature reduction (Lu et al, 1985).

In the blast furnace process pellets are charged from the top with layers of coke in between. Hematite is step wise reduced to magnetite, wüstite and finally metallic iron that melts and is tapped at the bottom. It is an ancient principle that is still dominating the ironmaking in modern times. In 1996 LKAB built a small scale experimental blast furnace (EBF) to develop, test and market new blast furnace pellets.

During the descent in the EBF the pellets are subjected to increasing temperatures and reducing conditions. They are further exposed to circulating alkali and dust. This circulation may cause build-up of scaffolds at the walls which can cause disturbances in the production.

A further attempt to improve the pellets is to add a thin coating of minerals. Coating on pellets was first tried on direct reduction (DR) pellets to prevent the clustering of direct reduced iron. In 1996 LKAB began coating DR-pellets with dolomite and today almost all DR-pellets are coated to avoid sticking and improve gas permeability during the solid state reaction of iron ore pellets to iron.

1.1 Aims of Study

The aims of this thesis are to: (i) describe the olivine reactions during reduction in the blast furnace, (ii) compare phases found in fast cooled probed pellets and slow cooled excavated pellets from the EBF, and (iii) report on the behaviour of different coating materials on blast furnace pellets.

1.2 Olivine Mineral

Olivine is the term for the orthorhombic M_2SiO_4 silicates where M = Mg^{2+}, Fe^{2+}, Ca^{2+} and Mn^{2+}. There are continuous solid solution series between the endmembers forsterite (Mg_2SiO_4) and fayalite (Fe_2SiO_4), and between kirschsteinite ($CaFeSiO_4$) and monticellite ($CaMgSiO_4$). There is rarely any solid solution between the two series (Klein, 2002). Forsterite has a melting temperature of 1890°C and lowers with increasing FeO content; pure fayalite melts at 1205 °C. LKAB adds forsterite with 7% FeO in their pellets which yield the formula $(Mg_{1.9}Fe_{0.1})SiO_4$.

1.3 Mineral Reactions in the Pelletising Process

The mineral reactions in LKAB's blast furnace pellets during the pelletising process have been thoroughly investigated by Niiniskorppi (2004). The Fe^{2+} in forsterite is oxidised to Fe^{3+} resulting in inclusions of hematite and silica in the forsterite core. Further a complex set of coronas are formed due to iron oxidation. The first corona consists of a two phase lamellar structure, each phase too small to examine individually with the optical microscopy or SEM used in the previous study. They are believed to be magnetite or magnesioferrite and a silica phase. Grains of magnesioferrite are embedded in an amorphous silica rich phase in the second corona. Between the coronas a layer is usually observed containing Ca-Fe-Mg-silicate of pyroxenitic composition. Magnesioferrite commonly occurs in hematite close to the olivine grains.

1.4 Alkali Cycle in the Blast Furnace

A recurring subject in the study of olivines in the blast furnace is alkali and in particular potassium. A study of the formation of potassium slag is given in Paper I.

When alkali is reduced it is gaseous at the temperatures found in the lower part of the blast furnace and it tends to rise, oxidise and deposit on the cold material descending, or on refractory lining. This circulation is known to cause serious problems with burden hanging in the furnace, and cause enhanced disintegration of the ferrous burden and coke, increasing the amount of fines in the furnace and thereby decreasing permeability causing gas channelling (Davies et al, 1978).

1.5 Effects of Quench Time on Pellets

At the end of each campaign the EBF, including the burden material, is quenched with nitrogen gas from the top. After a cooling period the EBF is excavated for samples of iron ore pellets, sinter, coke material etc. An alternative method for removing burden material *in situ* from the EBF is through cylindrical water-cooled probes. The probes are situated in the upper- and lower shaft region where the temperature of the burden material during operation is 800-900°C and 900-1100°C respectively. The quench time of the probe materials is much faster than for the excavated materials.

Kinetics at these high temperatures are considerably rapid (Biswas, 1981) since diffusion still plays an important role. There are several aspects to consider in characterising kinetic phenomena in the pellets; reduction degree, microstructures, morphology and micro scale reaction related to diffusion. These have been investigated in this thesis work.

A model for the quench time of the EBF was developed by BlueScope Steel using the gas flow, heat transfer and permeability components of BlueScope Steel's proprietary two-dimensional steady-state numerical model of the blast furnace, called 'SHAFT' (Chew et al, 2001). In the model the N_2 flow was assumed to be 100 m^3/h. The model shows a cooling time of three hours from 800°C to 500°C in the upper shaft of the EBF. In the lower shaft it takes fifteen hours to cool from 1000°C to 500°C.

1.6 Effects of Coating on Pellets

A previous study with coating of olivine, dolomite and quartzite on LKAB olivine blast furnace pellets have shown a decrease in dust generation, prevention of sticking and higher gas utilisation with a smoother blast

furnace operation. The coating of pellets was considered to be a significant improvement in optimising the blast furnace operation (Sterneland and Jönsson, 2003).

2. Methodology

Oxidised pellets used in this study were collected from the cooler in LKAB's pelletising plant in Malmberget. The reduced pellets were collected from the EBF from both excavation and probing of five different campaigns. The outline of the EBF with the location of charging level, probes and tuyeres are presented in Figure 1 (a). The samples have further been collected from the wall and centre of the cross section of the blast furnace burden as shown in Figure 1 (b). The pellets are described with three main zones; core, mid-radius and shell as presented in Figure 1 (c).

The pellets samples were cast in Epofix resin, cut, polished and examined with reflected light optic microscopy. Further microprobe analysis was performed with a Cameca SX50 equipped with three wavelength dispersive spectrometers (WDS) and a backscatter electron (BSE) detector. A scanning electron microscope (SEM); a Philips XL30 equipped with an energy dispersive spectrometer (EDS) and BSE detector was also utilised. The WDS is calibrated against various standards and the EDS is calibrated against Cu. The spot size for both the microprobe and SEM is 1-5 µm. The microprobe and SEM are used to assess the chemical composition and study morphology of phases.

An automated SEM – QEMSCAN® – was used for quantitative studies over a larger number of pellets and larger surface per pellets than can be achieved with manual SEM. It combines the power of four liquid nitrogen-free EDS detectors, an integrated hardware platform and an advanced software package for identification and quantification of minerals and other phases. The instrument combines both BSE-values and X-ray spectra to identify minerals and phases. The QEMSCAN® measurements performed on the olivine blast furnace pellets used the FieldScan mode of analysis. This measurement mode maps each field, using a user-defined spacing between measurement points. All fields analysed in one sample are subsequently stitched together to form a single mosaic image of the whole area analysed.

The study focused on the alteration phases and slag phases within the pellets. Pellets from eleven excavated pellets layers, and three different horizontal positions in the EBF were analysed using FieldScan measurement mode with a point spacing of 7 µm. A total of 198 pellets were measured. To optimise the measurement time a strip of one third of the pellet in width was measured along each pellet, divided in five fields according to Figure 2.

A mineral database for pellets samples was developed for the QEMSCAN® study with a set of defined slags, i.e. slags where X-ray spectra was collected and the composition was determined. These slags are named after there dominating elements, e.g. *Slag 2 FeSi* is an iron containing silicate slag. However, a large number of phases containing potassium presumed to be glasses or slags were not defined due to the tedious work of collecting X-ray spectra for all varying compositions. Two different models were developed to describe them; one model describes the potassium content (in wt%) in given intervals and a primary focus is the separation of silicate slags (*K Slag Si*) from the non-silicate iron slags (*K Slag Fe*). Thus, the first slags must contain at least 5 wt% silica. The latter slags must contain iron and have no or low amounts of silica. Any other elements are allowed in any concentration.

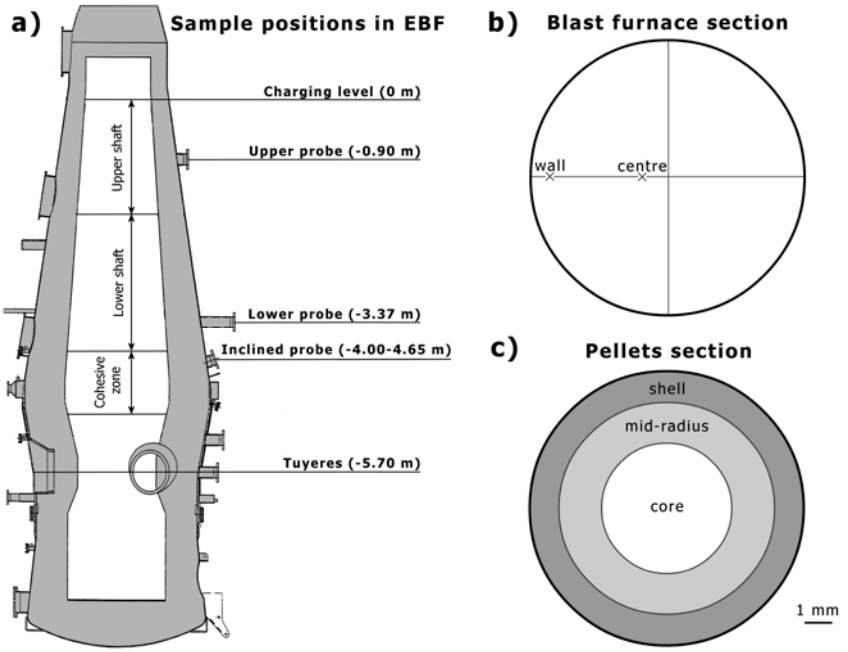

Figure 1. (a) The location of charging level, probes and tuyeres in the experimental blast furnace. (b) The position of the wall and centre in cross section of the blast furnace shaft. (c) Zones within the pellets.

The second slag model separates the potassium-bearing silicate slags and describes what general elements they are associated with. These entries were designed with the requirement that the essential elements are present in a considerable amount and the non-essential elements are restricted to minor amounts. The elements referred to are Si, Al, Ca, Mg and Fe. K and Si are defined as essential in all entries but K is also allowed in minor amounts.

A database for the olivine solid solution was also developed for QEMSCAN® measurements.

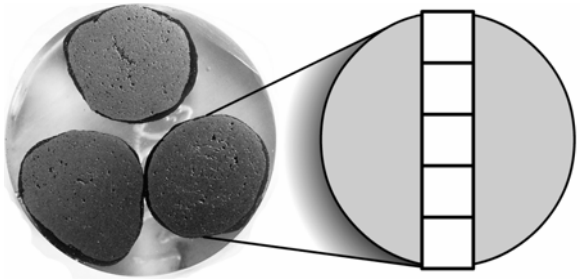

Figure 2. A photo of a prepared sample block with three pellets (left) and a schematic view of the QEMSCAN® measurement area within a pellet divided into five fields (right).

Micro-Raman spectroscopy was utilised with Kaiser's HoloSpec imaging spectrometer equipped with thermoelectrically cooled charge-coupled device detector (Andor). It uses an argon ion laser as a light source with the wavelength 415 nm (green light) and maximal effect of 50 mW. Spectra were collected from -220 to 2300 cm^{-1} and the measurement time was about five minutes. The spot size of the micro-Raman instrument is not smaller than for the SEM (~5 μm) but will yield further structural information if there are several phases present on a small surface.

Micro-Raman spectroscopy involves the use of light to probe the vibration behaviour of molecular systems. Vibration energies, or bonding energies, in molecules and solids are in the range of 0-60 kJ/mol or 0-5 000 cm^{-1}. This corresponds to the wavelengths of visible light. In a micro-Raman experiment the molecular vibrations are studied in a scattering experiment where the energy of an incident light beam is slightly raised or lowered by inelastic interaction with the vibration modes. The spectroscopy gives rise to a set of scattering peaks as a function of energy representing the different interaction from the different modes (McMillan and Hofmeister, 1988). The method will aid in the determination of the crystallinity or non-crystallinity of phases too small to determine with SEM.

Mössbauer spectroscopy or nuclear gamma resonance spectroscopy was utilised to determine the reduction degree of selected samples from the EBF. A resonant absorption experiment involves recoil free emission and absorption of photons from a radioactive source and an absorber (the sample) in such a way that the absorbing nuclei represent the exact energy state as the emitted photon. This spectroscopy method, due to the principally simple instrumentation rapidly becomes an important method in solid-state physics, chemistry and earth sciences especially for iron, an easy accessible isotope for resonant absorption in solids (Bancroft, 1973). The resonant experiment is built around a radioactive source, in the case of iron samples, ^{57}Co mounted in a metallic rhenium foil. The ^{57}Co decay to ^{57}Fe, a stable

isotope occurring in natural iron (2 atomic-%), and emits γ~–radiation of different energies, one of which is electronically selected for resonant absorption experiment (14.4 keV). The photon energy has to be varied to obtain the required energy differences between the different energy levels of ^{57}Fe in the absorber sample for resonant absorption. This is performed by mounting the source on a vibration device accelerating the source towards the absorber sample and utilizing the Doppler effect for modulating the photon energy. A Mössbauer experiment thus measure at which acceleration velocity, proportional to the energy, resonant absorption occur. A sharp absorption line is observed. In fact the absorption is so sharp that it is sensitive to very small changes in the bonding energy, of the order of 10^{-9} eV, which makes Mössbauer spectroscopy a very powerful tool for investigation of iron containing solids. The main spectrometer devices are the vibrator with the source, a powder or thin film absorber, a detector and a multi channel analyser (MCA) for storing the pulses.

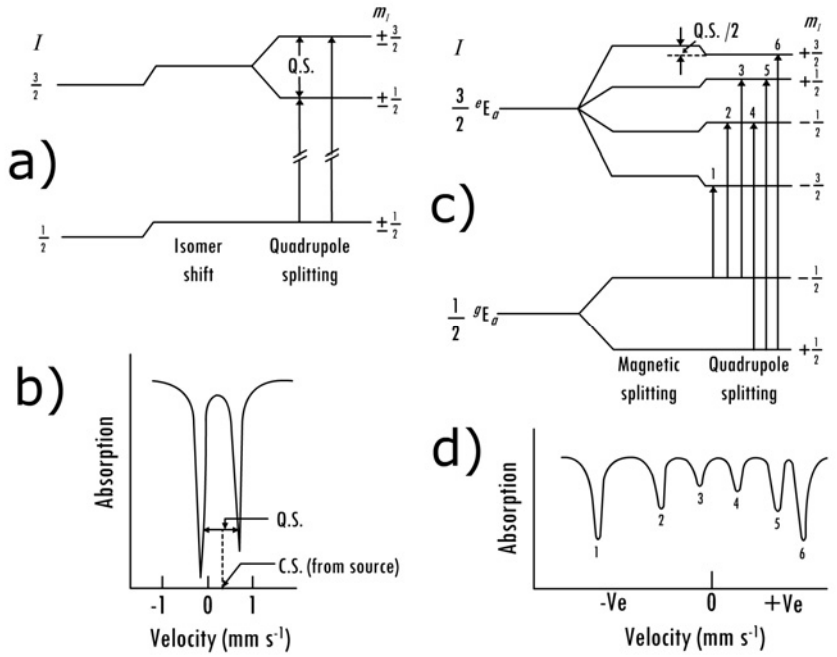

Figure 3. (a)-(b) Nuclear energy levels and quadrupole splitting in Mössbauer spectroscopy: (a) Absorber energy levels (I=3/2) split into two by quadrupole interaction. (b) Resulting Mössbauer spectra. (c)-(d) Combined magnetic and quadrupole splitting: (c) Energy level diagram for magnetic and quadrupole interaction. (d) Resulting Mössbauer spectra.

The shape of Mössbauer spectra from ^{57}Fe in the solid depends on the electronic and nuclear properties of iron. The nuclear properties are in the quantum theory defined by the nuclear spin values *I* with possible values *I-1…-I*. E.g. iron with spin of 1/2 has two possible m_I; 1/2 and -1/2, i.e. the ground state, and spin values of 3/2 and -3/2, i.e. the excited state.

Possible transitions for a paramagnetic solid are indicated in Figure 3 (a) giving rise to a shift relative to the source, the so called *isomer shift* and a splitting of the single absorption doublet – *the quadrupole splitting* in Figure 3 (b). For magnetic splitting the iron nucleus feel a hyperfine field and six transitions are allowed resulting in a six-line pattern shown in Figure 3 (c) and (d).

Isomer shift values are a measure of the electron configuration and thus determined by the valence state Fe^0, Fe^{2+} and $Fe^{3+} \approx 0$, ≈ 0.35 and ≈ 1.0 mm s^{-1} respectively relative to metallic iron; an often-used calibration substance of the velocity scale. Also non-integral valence state are observed e.g. in magnetite Fe_3O_4 with an intermediate isomer shift of 0.67 mm s^{-1} for octahedral coordinated Fe indicative of valence state of +2.5 indicating fast electron hopping at room temperature. Quadrupole splitting is determined by the electrical field gradient around the iron nucleus and bear information on crystallographic aspects of the chemical bonding e.g. crystal geometry of the coordination polyhedral. For an isotropic bonding symmetry the quadrupole splitting will vanish resulting in single line absorption, e.g. the cubic iron oxide wüstite (FeO).

Intensities of the Mössbauer absorption lines are in general proportional to the concentration of iron in the respective crystallographic sites in solids and qualitative and quantitative information can be obtained from Mössbauer parameters from computer fitted spectra. Since the ^{57}Fe Mössbauer spectroscopy is highly selective analytical method only iron containing phases will be seen in the spectra from a multi phase sample. Observe that magnetic split spectra have intensity ratios 3:2:1:1:2:3 for the six line absorption pattern in Figure 3 (d). The velocity range between the outermost lines define the nuclear hyperfine field and depends strongly on the electro configuration, e.g. Fe^{3+} with five unpaired d-electrons has a larger field compared to Fe^{2+} ions further contributing to the determination of oxidation states of iron in iron oxides.

3. Olivines in oxidised pellets

The olivines in oxidised pellets have previously been described in depth by Niiniskorpi (2004). However, some phases are too small for analysis with SEM utilised by him in that study. The inclusions in the forsterite core, previously assumed to be hematite, and the two phase lamellar corona (first corona) and surrounding silicate phase and iron oxide (second corona) were subjected to micro-Raman analysis in this study presented in Paper V. The resulting spectra are compared with previously measured modes for hematite, magnetite, magnesioferrite, orthoenstatite, forsterite and vitreous silica (Chopelas, 1991; Geissberger and Galeener, 1983; Gasparov et al, 2005; Lin, 2003; McMillan et al, 1984; Shebanova and Lazor, 2003; Shim and Duffy, 2002; Wang et al, 2002 and Winell et al, 2006). Some of the possible phases in this study have Raman modes that overlap in the literature, but through studying the most intense modes the method can be used to identify the phases.

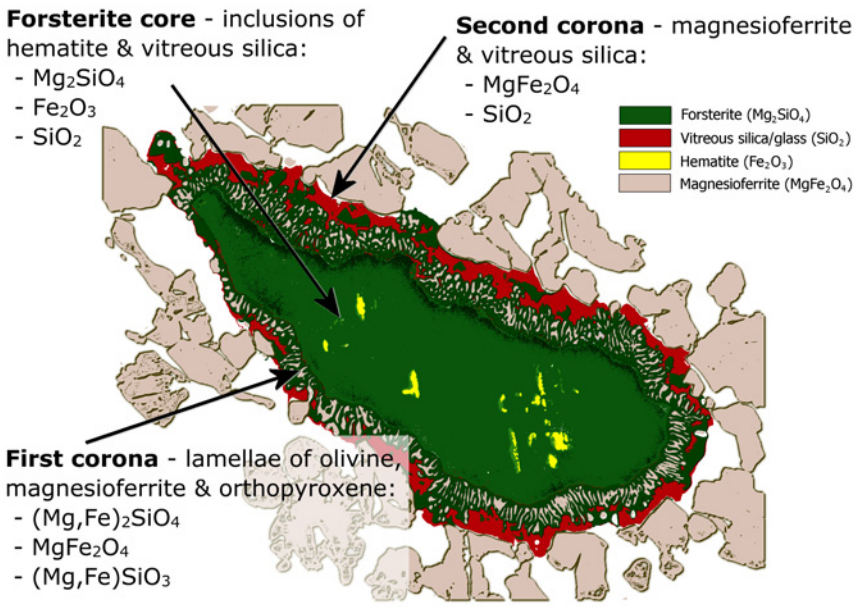

Figure 4. Digitally colored backscatter image from point analyses by WDS. Forsterite core with reaction coronas from oxidised pellets. Phases determined with WDS and micro-Raman spectroscopy.

In the forsterite core with inclusions the micro-Raman spectra matches that of forsterite, hematite and vitreous silica in accordance with literature. The vitreous silica in the micro-Raman is indicative of having a phyllosilicate structure – $Si_2O_5^{2-}$. These phases are schematically presented in Figure 4.

The first corona contains secondary formed olivine, magnesioferrite and orthopyroxene. The phases are too small to determine the ratio of iron and magnesium in the respective phases through SEM. The second corona consists of magnesioferrite and vitreous silica.

4. Olivines in reduced pellets

The reactions of the olivine phases found in the reduced pellets are described in Paper I – lower shaft and cohesive zone, and in Paper V – upper and lower shaft, and cohesive zone. The primary olivine with composition $(Mg_{1.9}Fe_{0.1})SiO_4$ is referred to as the *forsterite core* in the present study. The rims of olivine are secondarily formed in the blast furnace process. The silicate phases that stem from the second corona in the oxidised pellets will be referred to as *glasses*. The crystallinity of these phases is difficult to determine even with the micro-Raman spectroscopy, especially in the upper shaft of the EBF.

The reduction degrees of the samples are estimated from optical analysis and are given schematically in Figure 5.

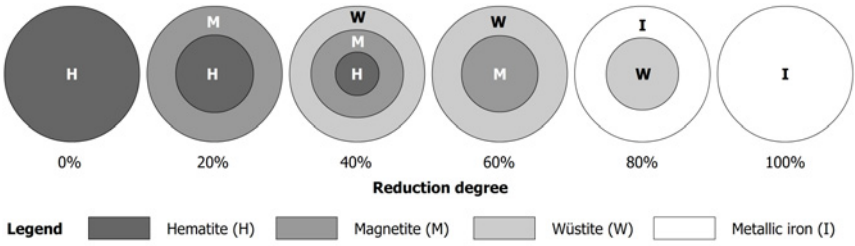

Figure 5. Schematic representation for the optical determination of the reduction degree of pellets from the EBF.

4.1 Upper Shaft of the Experimental Blast Furnace

The reduction degree in the upper shaft goes from 0% up to 80%. In some EBF campaigns there has been build-up of scaffolds in the upper shaft. Pellets found inside scaffold have a reduction degree of 100% due to longer residence time in the blast furnace.

The Fe^{3+} in magnesioferrite in the first and second corona from the oxidised pellets becomes unstable in the blast furnace's reducing gas. In the reduction step from hematite to magnetite in the pellets the Fe^{3+} in the second corona will be reduced to Fe^{2+} and expel magnesium to react with the vitreous silica as described in Equations 1 and 2. Potassium gas can also

work as a reducing agent and form $K_2O{\cdot}4SiO_2$ glass according to Equation 3. The second corona remains but absorbs various elements, e.g. aluminium, potassium, magnesium, iron and calcium, cf Figure 6.

$$3MgFe_2O_4 + 1.5SiO_2 + CO_g \rightarrow 2Fe_3O_4 + 1.5Mg_2SiO_4 + CO_{2,g} \quad [1]$$

$$3MgFe_2O_4 + 3SiO_2 + CO_g \rightarrow 2Fe_3O_4 + 3MgSiO_3 + CO_{2,g} \quad [2]$$

$$3MgFe_2O_4 + 7SiO_2 + 2K_g \rightarrow 2Fe_3O_4 + 3MgSiO_3 + [K_2O{\cdot}4SiO_2] \quad [3]$$

In the first corona the magnesium from magnesioferrite will enter the orthopyroxene and form olivine according to Equation 4.

$$3MgFe_2O_4 + 3MgSiO_3 + CO_g \rightarrow 2Fe_3O_4 + 3Mg_2SiO_4 + CO_{2,g} \quad [4]$$

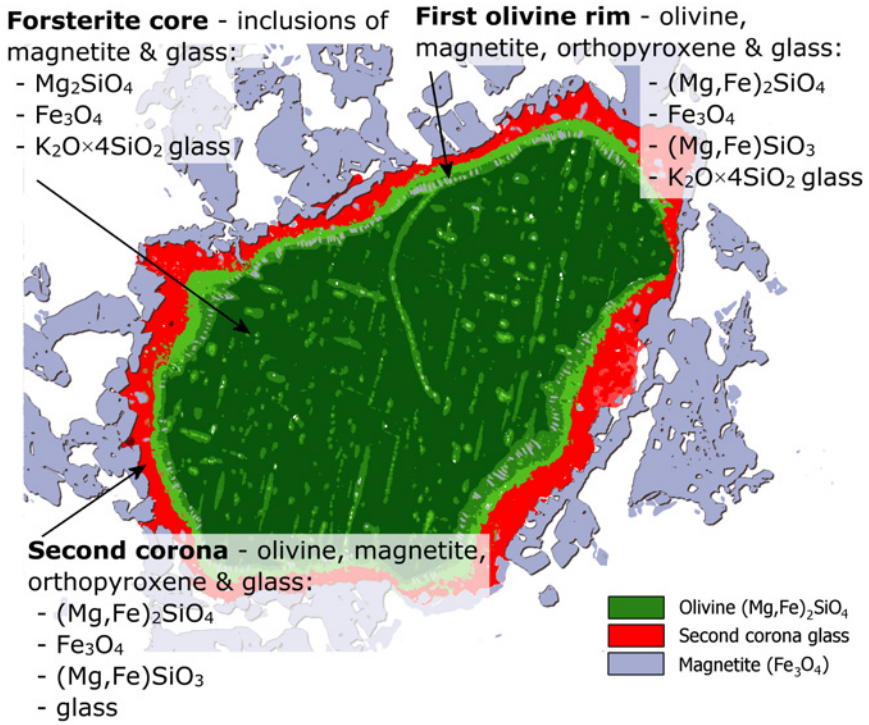

Figure 6. Upper shaft of the EBF at 40-60% reduction - digitally colored backscatter image from point analyses by WDS. Forsterite core with inclusions surrounded by the first olivine rim and second corona. The magnetite surrounding the silicate phases may contain minor amounts of magnesium. Phases determined with WDS and micro-Raman spectroscopy.

The phases in the first corona appears to be merging but with the magnetite lamellae still visible. This is called the *first olivine rim* shown in Figure 6.

The surrounding magnetite contains lower amounts of magnesium than the magnesioferrite found surrounding olivines from oxidised pellets.

The glass phases found in the second corona vary in composition and it is possible to classify them in four glass groups presented in Figure 7. The glasses in the second corona in contact with the first olivine rim mainly have a pyroxenitic composition like glass classes 2, 3 and 4 in Figure 7. With further reduction of magnetite to wüstite in the pellets this glass will react with the first olivine rim phases and form the second olivine rim containing olivine that is more iron rich than the primary forsterite core, see Figure 8. Any calcium or alkali that was in the glass will be left as glass inclusions in the second olivine rim. Equation 5 describes the merging of the second corona and the first olivine rim. The second corona is given with *Glass 2* composition. The Fe^{3+} in magnetite is completely reduced.

$$Fe_3O_4 + 6Mg_2SiO_4 + 3(Mg_{0.8}Fe_{0.2})SiO_3 + CO_g \rightarrow 9(Mg_{1.6}Fe_{0.4})SiO_4 + CO_{2,g} \quad [5]$$

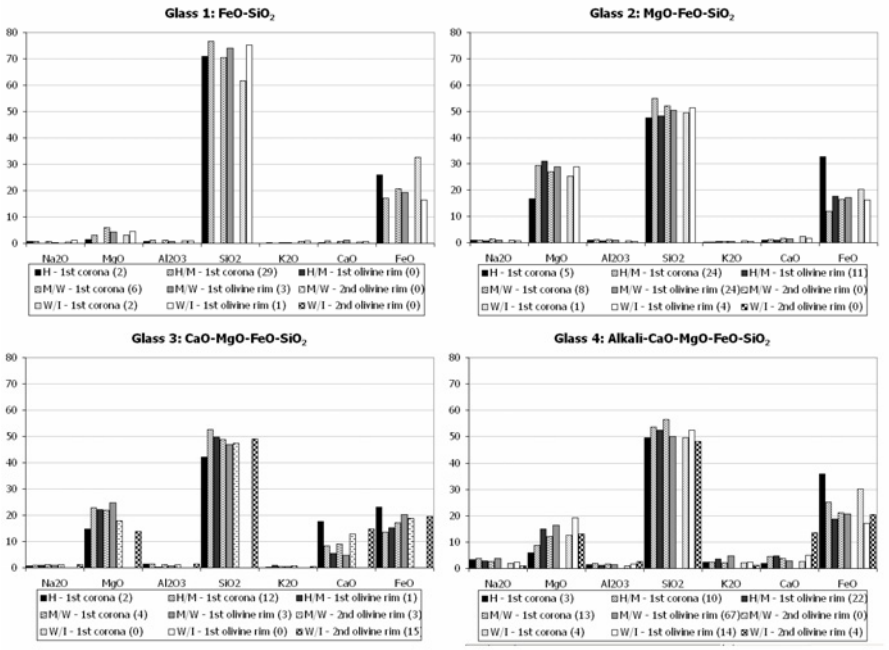

Figure 7. Upper shaft of the EBF: Classification of glass phases found in the second corona or as inclusions in the second olivine rim. The values are means of a number of analyses and given in wt-%: Glass 1 = 43 analyses, Glass 2 = 77 analyses, Glass 3 = 40 analyses and Glass 4 = 137 analyses. Methods of analyses are WDS and EDS.

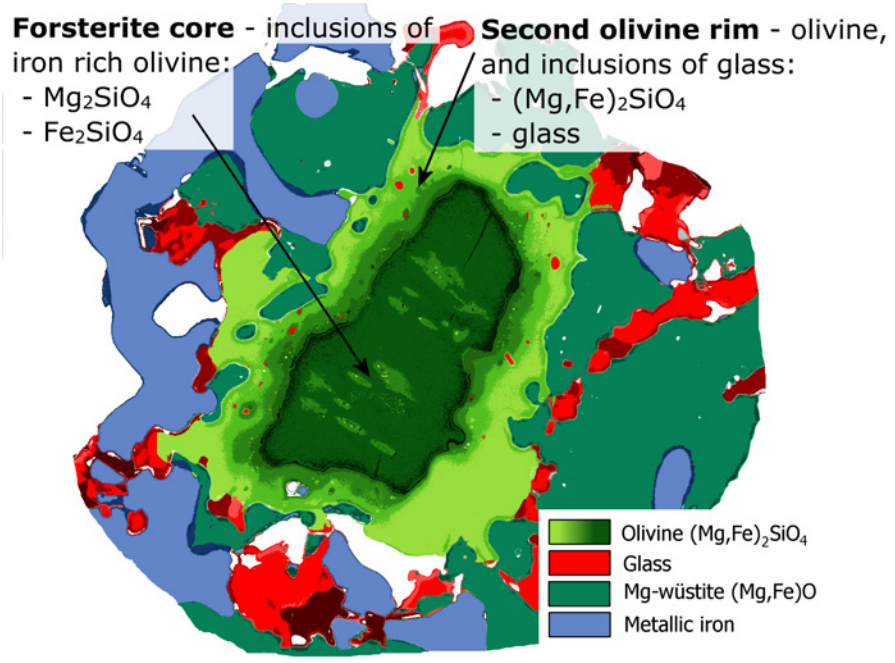

Figure 8. Upper shaft of the EBF at 80% reduction - digitally colored backscatter image from point analyses by WDS. Forsterite core with inclusions surrounded by the second olivine rim with glass inclusions. The wüstite surrounding the silicate phases contain about 5 wt-% MgO. Phases determined with WDS and micro-Raman spectroscopy.

4.2 Lower Shaft of the Experimental Blast Furnace

The degree of reduction in the lower shaft is 80-100% and the temperature is 750-1100°C. The olivines found in the lower shaft generally have the second olivine rim in Figure 8. The rim is wetting completely against the surrounding wüstite allowing for diffusion of magnesium and iron.

At the wall of the EBF at the level of the lower shaft some olivines appear with a cracked glass rim shown in Figure 9. Micro-Raman measurements of the cracked glass rim show that it retains the orthosilicate close-order structure but is disturbed by the entrance of potassium. It appears cracked due to fast quenching.

The glasses found in the immediate surroundings of the olivines in the lower shaft absorb more alkali and appear more complex than in the upper shaft, see Figure 10. More glasses contain alkali with increasing reduction degree, and the amount of alkali in each glass increase as well.

In pellets with a thick metallic iron border surrounding the wüstite core there are generally no olivines left inside the core. Completely metallic

pellets are also found with olivine free cores, however the olivines remain in the shell of pellets. The reduction gas is slowed down by the thick metallic iron border that is formed around the wüstite core. When the temperature increases the diffusion of magnesium from olivines into wüstite increases as well. This reaction is described in Equation 6.

$$(Mg_{1.9}Fe_{0.1})SiO_4 + (Mg_{0.07}Fe_{0.93})O \rightarrow (Mg_{1.77}Fe_{0.23})SiO_4 + (Mg_{0.2}Fe_{0.8})O \quad [6]$$

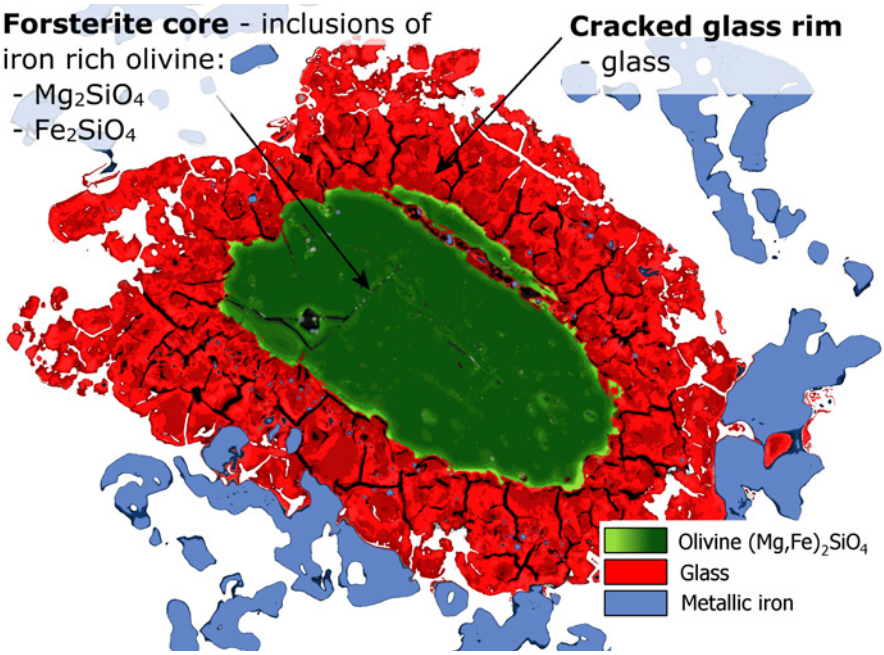

Figure 9. Lower shaft and wall position of the EBF - digitally colored backscatter image from point analyses by WDS. Forsterite core surrounded by the cracked glass rim. Phases determined with WDS and micro-Raman spectroscopy.

The increasing amount of magnesium into the wüstite delays its reduction to iron further with the formation of magnesiowüstite (Harkki, 1980). Magnesium can keep diffusing out of the olivine making it more iron rich as long as the magnesiowüstite is present. The olivine will react with potassium and aluminium gas and form glass, shown schematically in Equation 7.

$$(Mg_{1.77}Fe_{0.23})SiO_4 + K_g + Al_g \rightarrow [K_2O{\cdot}0.3Al_2O_3{\cdot}0.5MgO{\cdot}FeO{\cdot}2SiO_2] \quad [7]$$

The reason why olivines are found in the metallic shell of pellets with olivine free cores is due to the faster reduction of wüstite to metallic iron.

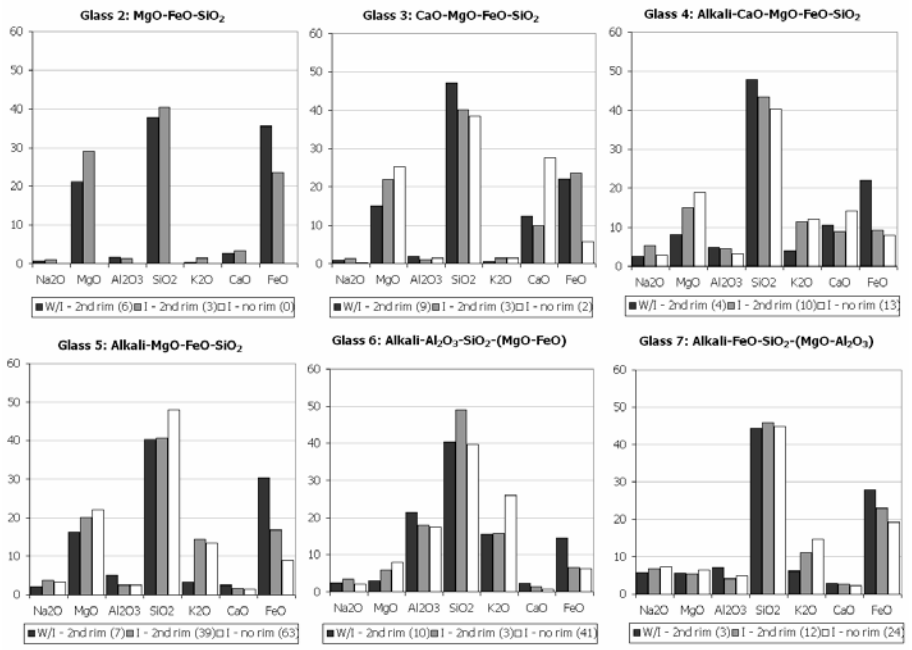

Figure 10. Lower shaft of the EBF: Classification of glass phases found outside the forsterite core; as inclusions in the second olivine rim (*2nd rim*) or as partial glass outside rim if present. The values (wt-%) are means of a number of analysis (see number in pranthesis). Method of analysis is WDS and EDS. W = wüstite, I = iron.

4.3 Cohesive Zone of the Experimental Blast Furnace

The degree of reduction in the cohesive zone is 80-100% and the temperature is 1100-1200°C. The Fe^{2+} in the second olivine rim becomes unstable with the increased reduction. The second olivine rim is reduced to metallic iron droplets, silica and iron free forsterite as it forms the third olivine rim shown in Figure 11. This reaction is presented in Equation 8.

$$5(Mg_{1.6}Fe_{0.4})SiO_4 + 2CO_g \rightarrow 4Mg_2SiO_4 + 2Fe^0 + SiO_2 + 2CO_{2,g} \qquad [8]$$

The free silica attracts potassium that is deposited from the furnace gas, furthering the reduction of iron. Eventually a glass will form out of the consumed forsterite core shown schematically in Equation 9. Figure 12 shows the near complete consumption of the olivine with only spots of forsterite left.

$$(Mg_{1.9}Fe_{0.1})SiO_4 + SiO_2 + K_g \rightarrow Fe^0 + [K_2O{\cdot}2MgO{\cdot}4SiO_2] \qquad [9]$$

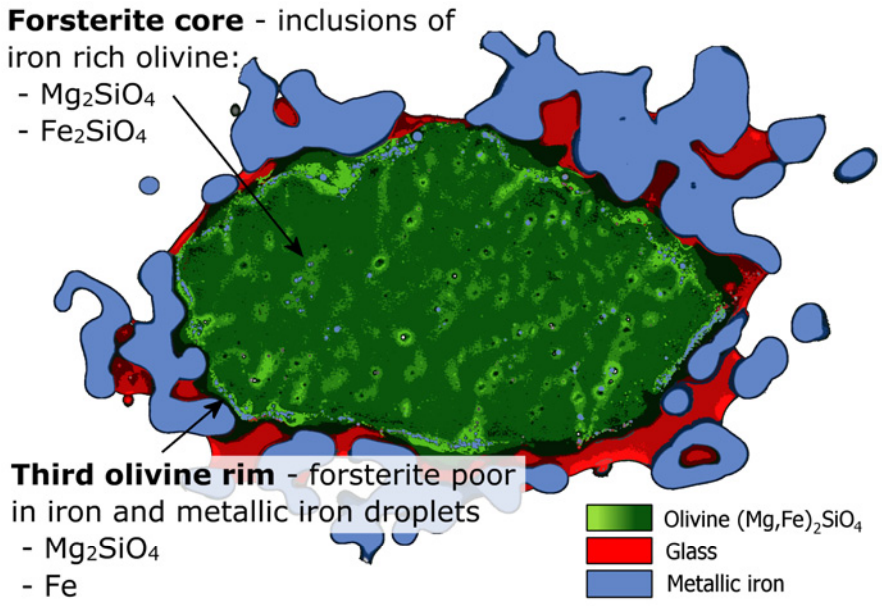

Figure 11. Cohesive zone of the EBF - digitally colored backscatter image from point analyses by WDS. Forsterite core surrounded by the third olivine rim. Phases determined with WDS and micro-Raman spectroscopy.

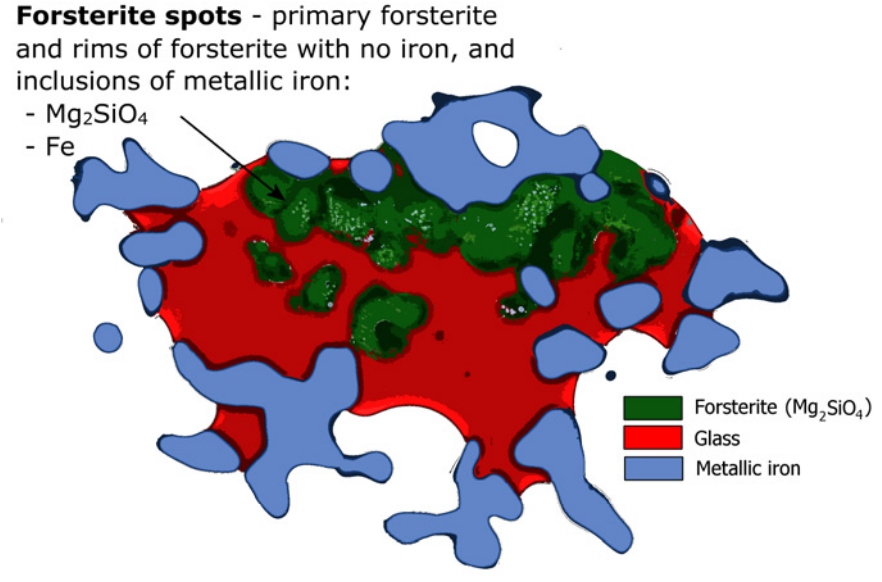

Figure 12. Cohesive zone of the EBF - digitally colored backscatter image from point analyses by WDS. Forsterite spots with inclusions of metallic iron and surrounded by rims of forsterite with no iron. Phases determined with WDS and micro-Raman spectroscopy.

4.4 Magnesium and Iron Reactions between Olivine, Glass and Iron Oxides

From the chemical analyses of phases presented in Paper V there are clear trends for the diffusion of magnesium and iron with increasing temperature and reduction in the blast furnace. These trends have been plotted in Figure 13 as the means of chemical analysis of FeO in all olivine rims and glasses, and MgO in the iron oxides divided into the degree of reduction of the pellets.

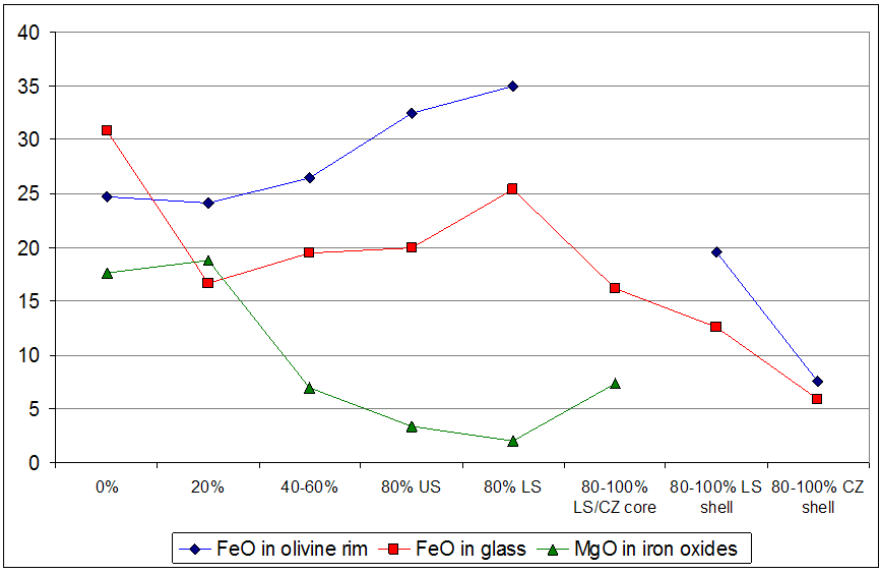

Figure 13. The mean values of chemical analysis (EDS and WDS in wt-%) of FeO in olivine rim and glass and MgO in iron oxides plotted with increasing reduction degree. Amount of analyses are: olivine rim = 385, glass = 594, magnesioferrite and Mg-wüstite found near olivine = 164 and Mg-wüstite in olivine free pellets core = 7. US = Upper shaft, LS = Lower shaft, CZ = cohesive zone.

The increase in FeO in olivin rim and glass are first governed by reduction up to the wüstite phase. In the wüstite phase magnesium and iron diffusion is controlled by the increasing temperature as the formation of magnesio-wüstite retards the further reduction to metallic iron.

When wüstite is finally reduced to metallic iron the reduction will once again control the olivine reactions. Potassium plays an important role in the olivine reactions throughout the EBF.

5. Quantitative study of olivine and slag in reduced pellets

The study of olivines with automated SEM – QEMSCAN® – gives quantitative data of the olivine reactions. Large pellets areas can be measured in short amount of time. This is useful to test the recurrence of observations made with manual SEM technique.

The relative amounts of the olivine phases in each excavated pellets layer and horizontal position is given in Figure 14. The green-blue phases are eight mineral compositions within the solid-solution series $Ca(Mg,Fe)SiO_4$ and $(Mg,Fe)_2SiO_4$. The yellow and ochre phases display *olivine slag*, described as the glasses in Figure 7 and 10. The olivine slags are divided based on if they have potassium. Note the phases described as slags in Paper II are still of undetermined crystallinity as the glasses previously described in this thesis. The terms slag and glass have unfortunately been used intermittently through the length of these studies.

The samples in this study collected in three horizontal positions shown in Figure 14, where position 0 is close to the wall of the EBF, position 1 is at the mid-radius and position 2 is in the centre of the EBF.

The absolute amounts of olivines – given with □ symbols in Figure 14, vary both between positions and pellet layers. Less olivine phases are present in position 0 (from 0.9 to 3.2 %) than in position 1 and 2 (from 2.0 to 4.5 %). The variation within the samples from the same position could be due to variations in porosity in the sample as the amounts are calculated as area percent.

At position 0 large amounts of potassium bearing olivine slag is present in pellet layers 13, 15, 19 and 25, which can be related to the high amount of potassium in the overall pellets at this position according to XRF analysis of crushed pellets samples as shown in Figure 15. The high amount of potassium in turn follows a high reduction degree for samples from position 0 as seen in Figure 16.

The occurrence of fayalite is related to reaction between iron oxides and silica rich phases such as forsterite. Pellets with relatively low reduction degree have high levels of iron oxide in the silicate phase. Therefore, fayalite and forsterite are the major phases in samples from position 1 and 2, while the amount of fayalite displays a decreasing trend with increasing furnace depth due to an increase in iron reduction. The high reduction degree in

samples from position 0, Figure 14, explains the smaller amounts of fayalite present in layers 4-15.

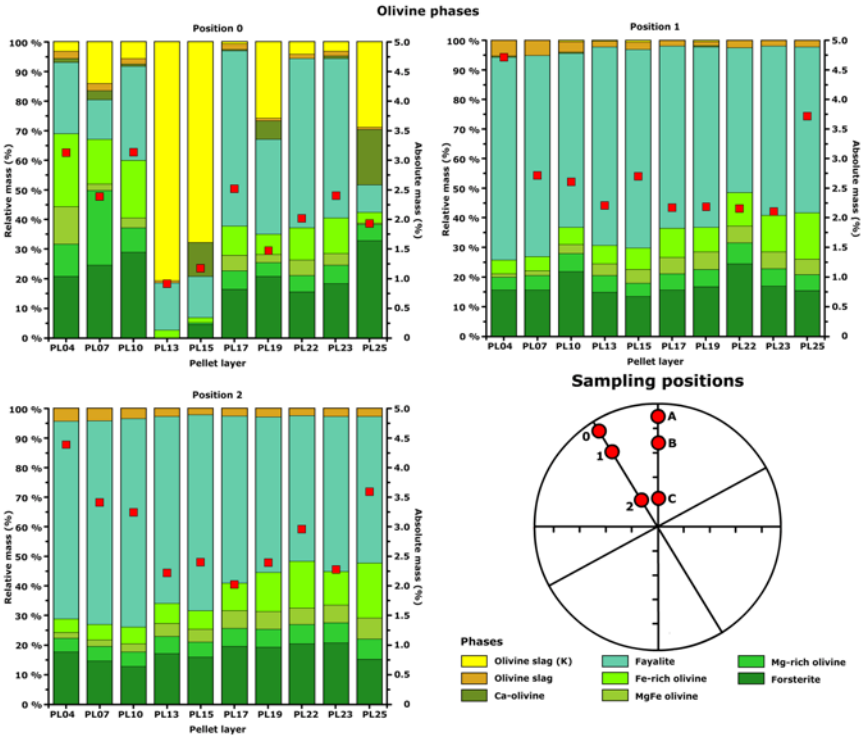

Figure 14. Relative mass-% of olivine phases for excavated pellet layers (PL) at three different horizontal positions in the EBF (0, 1 and 2), measured with QEMSCAN®. Red squares give the absolute mass-% of the whole measured area. Circle diagram shows the horizontal positions in the cross section of the EBF.

The amounts of *MgFe olivine* and *Fe-rich olivine* increases with depth in the furnace, indicating that olivine reacts with the surrounding iron oxides at increasing temperature in the blast furnace in accordance with observations through manual microprobe techniques.

The model describing the undefined slags serves to show the potassium content (in wt%) in given intervals. The relative amounts of potassium in the undefined slags for positions 0, 1 and 2 are given in Figure 17 (*K-slags Fe and K-slag Si)* along with defined slags (*Slags 1-22*), *Olivine slag (K)* and potassium bearing chlorite. The potassium mainly exist in low concentrations in *K-slag 1 Fe* and *K-slag 1 Si* at all positions. The non-silicate *K-slag 1 Fe* is more common at position 0 and in the pellets layers at a greater depth in the EBF at position 1 and 2. The slags with higher concentrations of potassium (*K-slag 2-3 Fe* and *K-slag 2-5 Si*) are more abundant at position 0 but increases with increasing depth for positions 1 and 2. Of the defined slags the phases *Slag 2 FeSi*, *Slag 10 KSi* and *Olivine slag*

(K) are dominating in position 0. In positions 1 and 2, *Slag 2 FeSi* is the most abundant potassium bearing phase, along with *Slag 5 SiFe*.

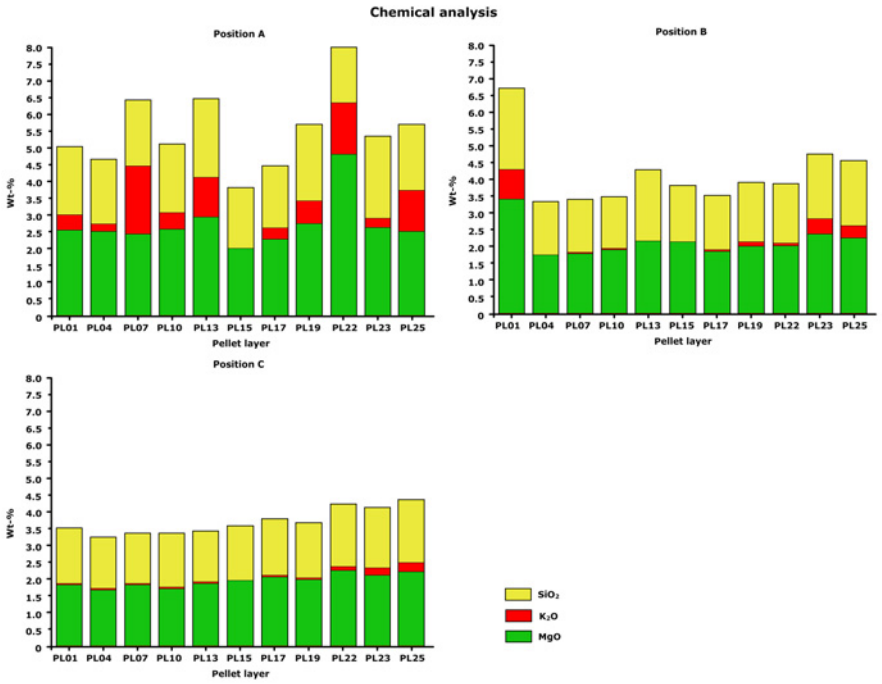

Figure 15. Chemical analysis by XRF in wt-% of crushed pellet samples at different excavated pellet layers (*PL*) at different positions (*A, B* and *C*, cf Figure 14).

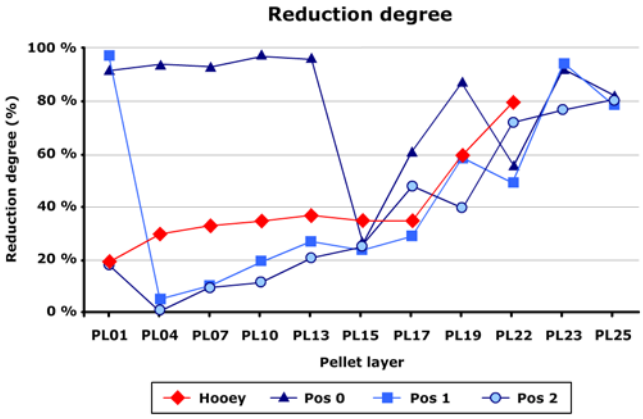

Figure 16. Reduction degree (%) at three horizontal sampling points (0, 1 and 2, cf Figure 14) plotted against the excavated pellet layers (PL) in the EBF. Compared against reduction data from Hooey (2004). Method of analysis was titration of iron ions (Fe^{2+}) and metallic iron.

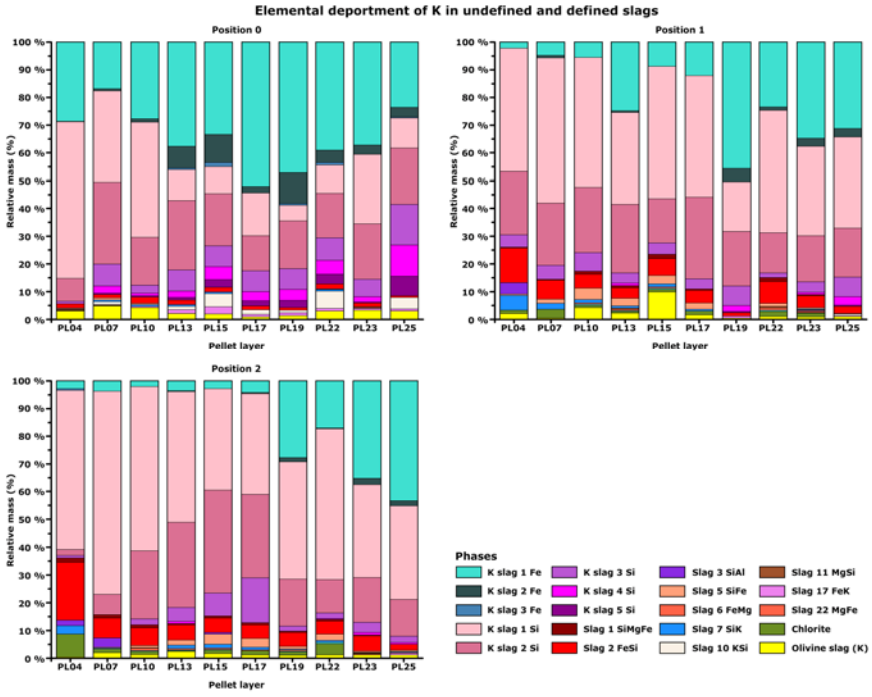

Figure 17. Relative amounts of potassium in slags

The use of semi-defined potassium slags helps to better define ~70% of the undefined potassium slags. According to this slag model the potassium in the undefined silicate slags is predominantly associated with iron and/or magnesium. This is in accordance with the observation of potassium glasses found around the olivine phases in Papers I and V.

6. Kinetics in reduced pellets

There are several physico-chemical conditions that change dramatically during cooling of the EBF burden. This will influence both the oxide and silicate phases as described in Paper IV.

Although this study is based on a limited number of sampled pellets the data will allow for qualitative conclusions to be made on the differences between probed and excavated pellets. Differences are small and irregular indicative of the establishment of a variety of local equilibrium conditions during operation of the EBF.

During quenching of the EBF it is expected that the reducing gases are vented out almost instantly because of the high nitrogen gas flow. This means that the reduction degree of iron oxide should be the same when comparing probe and excavated materials. However, the excavated material has been exposed to high temperature much longer time than the probed material, and it cannot be ruled out that some reducing gas is still remaining in the pellet layers, in cavities or in the interior of the pellets. As the oxygen content in the nitrogen gas is extremely low, the flushing of the gas during cooling should not contribute to any oxidation of the material.

The whole burden sunk about one meter during the quenching period. Some mixing of pellets with a low reduction degree, from layers higher up in the furnace, with pellets at lower positions where the samples were collected cannot be excluded. The probes, when working properly, will be filled with burden material from the interior of the EBF, from one wall to the other. Some mixing of pellets from adjacent horizontal positions in the burden can occur inside the probe.

Slight changes in process conditions in the EBF between the probing period and the shutdown of the process could also affect the overall material behaviour in the furnace.

The appearance of exsolved magnetite lamellae in wüstite in excavated pellets is a result of the slow cooling. With cooling non-stoichiometric wüstite is slowly growing out of its temperature stability region (Darken and Gurry, 1953). The wüstite with exsolved magnetite has the composition $Fe_{0.95}O$. The wüstite in the excavated pellets is just outside of the border of the stability region for single-phase within the wüstite-magnetite field. However, wüstite from probed samples has the composition $Fe_{0.93}O$, within the homogeneous wüstite field.

The forsterite cores and olivine rims change according to the reduction degree. There is no conclusive evidence to suggest that the differences in olivine morphology or composition observed between excavated and probed pellets are caused by the different cooling times.

There is also nothing that suggests the cooling time have any effect on the glass phases appearing in the upper shaft. Observations of the development of glass phases in the excavated and probed samples show that they rather follow the reduction degree of the pellets.

The differences in glass composition and distribution between probed and excavated pellets in the lower shaft can be connected to the quench time. The cooling of the alkali rich gas in the lower shaft will result in an alkali deposition in pellets that would not have been there if the pellets were probed.

Cracked glass around forsterite cores from the lower shaft (cf Figure 9) is an effect of fast quenching and is not found in the excavated pellets. Further observations are diffuse reduction fronts for the excavated pellets for both upper and lower shaft of the EBF.

7. Coating

A desirable phase to achieve with coating with regards to binding alkali is kalsilite – a relatively stable mineral in the blast furnace.

Five periods with different coating materials were conducted in the EBF in the order 1) kaolinite, 2) bauxite, 3) reference uncoated pellets, 4) olivine and 5) limestone. The samples were collected through probing of the EBF at the upper and lower shaft.

7.1 Upper Shaft of the Experimental Blast Furnace

Optical microscopy revealed 80% distribution of the coating materials with a mean thickness of ~20-40 μm, see Figure 18 (a). Coating assembled in a few larger clusters with a thickness up to 200 μm was found on each pellets. No minerals or slag were found on the surface of the reference uncoated pellets.

Negligible reactions have occurred in the upper shaft and the chemical composition were observed reflecting the original coating material e.g. primary olivine in olivine coating, corundum in bauxite coating and calcite in limestone coating were commonly observed. Calcite and dolomite are close to their decomposition temperature in the upper shaft but are stabilised by an increased CO_2 pressure.

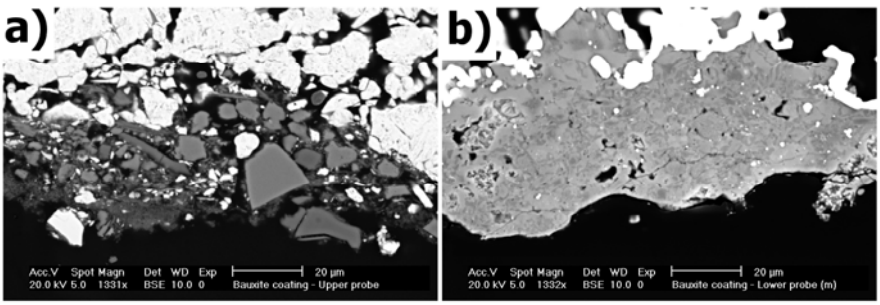

Figure 18. Backscatter images of coating from (a) upper shaft and (b) lower shaft. Dark phase is plastic, grey phase is coating material and light phases are iron oxides in the upper shaft and metallic iron in the lower shaft.

7.2 Lower Shaft of the Experimental Blast Furnace

Microscopy examinations showed more homogenous phases compared to the upper shaft samples, see Figure 18 (b). Around 15-25% of the pellet surfaces from the centre position in the EBF were covered by a slag phase regardless of the coating material including the reference uncoated pellets. The thickness varied from 20-200 μm.

Pellets at the wall had more surface slag; for the kaolinite coating over 90% of the pellets' surfaces were covered, for bauxite the pellets were covered 50-95%. Limestone and olivine coated pellets had coverage of 25-100%. For the reference pellets it was observed that 25-90% of the pellet surfaces were covered with slag phases close to the wall of the EBF.

From observations of coatings it is obvious that significant changes and reactions have occurred in the lower shaft. Extensive melting is obvious from the commonly observed glass phases. Furthermore, these samples differ in chemical composition depending on the horizontal position in the blast furnace where the wall samples had higher amount of alkali.

It is clear that all coated and uncoated pellets have surface phases within the system SiO_2-K_2O-Al_2O_3. The aluminium-silicate phases at the wall position are more potassium rich. The appearance of kalsilite on the uncoated pellets makes the use of coating redundant for binding alkali from a quality perspective. However, studies should be made determining the quantity of this phase formed with different coatings.

The reference pellets had surface slag phases most common in the system FeO-K_2O-SiO_2 at a FeO content >10%. These phases were usually found to be embedded in the metallic iron and went quite far into the pellet; probably originating from the interaction between slag and iron. Phases within this system have low melting points (Roedder, 1952). This would lead to a higher degree of sticking early on in the blast furnace. Due to the low melting point of these phases the potassium could easily re-circulate as has been shown with molecular dynamics simulations of potassium silicate glasses (Garofalini, 1983). The main advantage of coating appears to be that less of this unstable phase was observed on the pellet surface.

8. Reduction of Iron Oxides Monitored with Mössbauer Spectroscopy

Mössbauer spectra from reduced pellets are well resolved for a detailed analysis of present iron compounds, oxides as well as silicate slag, and allow quantitative conclusions of oxides ratios and solid solutions. A plot of mineral oxides with depth is depicted in Figure 19.

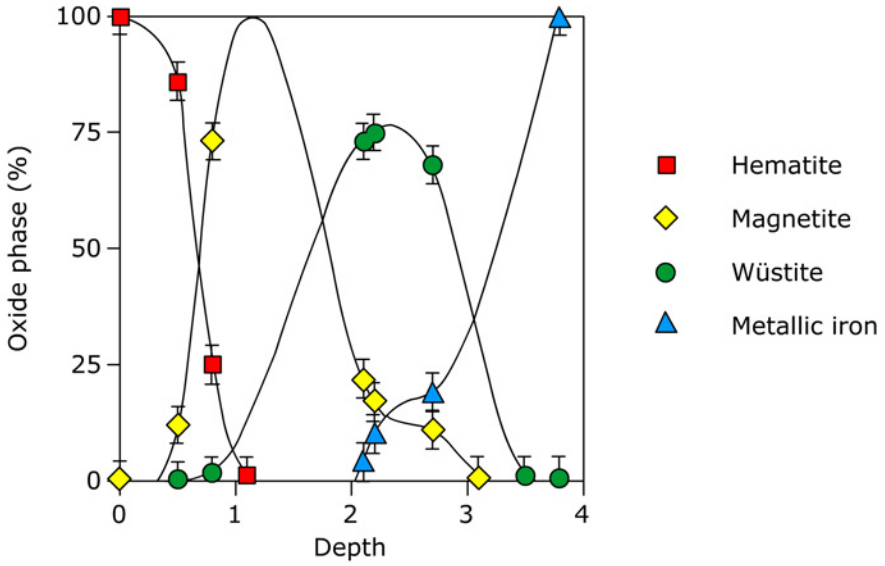

Figure 19. Modal mineral composition of reduced pellets from Mössbauer spectra.

9. Summary of the Papers

Paper I
9.1 Formation of Potassium Slag in Olivine Fluxed Blast Furnace Pellets

Mineralogical evaluation of olivine pellets coated with kaolinite, taken from the LKAB experimental blast furnace, shows significant reactions with potassium. Sampling has revealed strong potassium deposition in pellets in the lower shaft close to the wall, but much less deposition towards the furnace centre. Iron reduction and the deformation of the pellets were enhanced in the zone of high alkali deposition. Thin sections of pellet samples were prepared to distinguish amorphous and crystalline slag phases for a better understanding of the formation of the potassium rich slag. Olivine breaks down to various extents to form a SiO_2–FeO–MgO–K_2O glass. The kaolinite coating shows strong reaction throughout the cross-section of the lower shaft to form kalsilite ($KAlSiO_4$) and K_2O rich glassy slag. Studies of thin sections of the slag products were shown to be very useful in separating amorphous phases such as the K_2O rich glass from the crystalline olivine rim.

Paper II
9.2 Investigation of Minerals and Iron Oxide Alterations in Olivine Pellets Excavated from LKAB Experimental Blast Furnace

For a better understanding of pellet behaviour in the blast furnace process, LKAB has started to use automated mineralogy for the characterisation and quantification of its iron ore products and pellets. A mineralogical evaluation of iron ore olivine pellets, taken from a test campaign in the EBF, has been performed. The studied materials were samples from excavated pellet layers through the entire EBF at different positions. A large number of iron ore pellets was analysed using a combination of automated mineralogy, using QEMSCAN®, and chemical analysis, using XRF. Important information about the performance of pellets in the blast furnace process, such as a quantitative description of mineral and iron oxide alterations at different temperatures, Fe-reduction and alkali deposition, was obtained.

Paper III
9.3 Behaviour of Coatings on Olivine Fluxed Pellets in Blast Furnace Reduction

Different coatings on olivine fluxed blast furnace pellets were examined in LKAB's experimental blast furnace, Luleå. The aim of coating is to decrease dust generation, prevent sticking and to bind alkali for smoother operation. The coating materials were kaolinite, bauxite, olivine and limestone. Uncoated pellets were studied for reference. Probed samples from upper and lower shaft were examined for coating reaction. Methods used were optical microscopy, SEM, microprobe and Raman spectroscopy.

Upper shaft (~740 °C): minor reactions occurred in the coating. The distribution of coating was >80% with a thickness of ~30 μm. The reference sample had no surface phase.

Lower shaft (~840-980 °C): a majority of the phases were amorphous, reflecting the original coating minerals. The distribution varied between 20-100% including the reference sample. The thickness was 20-200 μm. Kalsilite occurred on all pellets including the reference; the use of coating for binding alkali is thus redundant from a quality perspective. The reference was more abundant in the FeO-K_2O-SiO_2 system; a low melting region mainly formed inside the pellets. The decreased sticking through the use of coating is likely a result of the coating hindering this low melting phase to spread over the pellet surface.

Paper IV
9.4 Effect of Quench Rate on Phases in Olivine Fluxed Blast Furnace Pellets

Samples from LKAB's experimental blast furnace (EBF) can be acquired through in shaft probing or excavation of the cooled burden. The difference in quench rate is considerable and the kinetic effects on LKAB's olivine fluxed blast furnace pellets are investigated. Probing of the burden was commenced shortly before quenching the EBF. Samples are from the upper and lower shaft with a subdivision of centre or wall samples in regards to the cross section of the burden column. SEM, microprobe and light optic microscopy were utilized for the analysis. Differences observed between excavated and probed pellets are mainly found in the lower shaft with e.g. the separation of wüstite into wüstite and magnetite due to wüstite growing out of its stability field during slow cooling of excavated samples. Diffuse reduction fronts in the pellets are observed for excavated pellets in both the upper and lower shaft but not in any of the probed pellets and is an effect of

a continued reduction during quenching, but not as aggressive as during EBF operation. There is higher alkali deposition in the olivine glass for excavated pellets in the lower shaft due to condensation of alkali gas upon quenching the EBF. The thick slag rim around olivines from probed pellets at the wall position in the lower shaft has cracks that are not observed in the excavated pellets.

Paper V

9.5 Olivine Reactions During Reduction in Blast Furnace Pellets

The use of olivine mineral as an additive in LKAB's blast furnace pellets has given the pellets great beneficial qualities in the blast furnace operation. This report aims to map out the olivine reactions on a micro scale as they descend in the blast furnace. The pellets have undergone reactions in an oxidating environment in the pelletising plant and the forsterites have developed a complex set of coronas before entering the blast furnace. The samples used in this study come from three different levels in LKAB's experimental blast furnace (EBF). Methods used are light optic microscopy, SEM equipped with EDS and WDS, and micro-Raman spectroscopy. Results show that the first and second corona from the oxidation will merge into one phase consisting of secondarily formed olivine with inclusions of glass. The iron content in the olivine rims will increase with increased reduction. Magnesioferrite solid solution will decrease with increasing reduction to magnetite. Magnesium solid solution will stabilize wüstite at increasing reduction degree and temperature. When reduction is commenced FeO in olivine is unstable and reduced out of olivine forming metallic iron droplets. The liberated quartz will react with potassium, further increasing the reduction and lowering melting points in the lower shaft where slag melting occurs. The olivine is consumed in the lower shaft at the wall position and in the cohesive zone in the centre position of the EBF, leaving a glass phase with varying composition.

Paper VI

9.6 Monitoring Reduction Degree of Olivine Fluxed Blast Furnace Pellets from Mössbauer Spectra

A study utilizing Mössbauer spectroscopy on reduced olivine fluxed blast furnace pellets has been performed on excavated samples from the LKAB experimental blast furnace (EBF). Mössbauer spectroscopy is resonant absorption of γ-rays in solids. It is a spectroscopy method particularly suited for absorption of iron containing compounds that can be performed at room temperature. Powder samples or in case of metallic iron thin plates were used in the analysis of pellets collected at different levels of the quenched

EBF. The evolution of reduction could be followed from well-resolved spectra obtained from successively reduced pellets even from multi-phase iron oxides samples. Characteristic Mössbauer parameters are given for the different oxides and quantitative values of mineral composition and their solid solution are gathered. Reduction degree for different layers is obtained from the computer fitted areas of the resonant envelopes and in good agreement with routine analysis. Identification of iron rich silica slag phases in the lower shaft is additional information from the Mössbauer spectra.

10. Concluding Remarks

The study of olivine, iron oxide and glass phases under reducing conditions in the blast furnace process has revealed that:

- In the reduction of hematite to magnetite in pellets from the upper shaft of the EBF the magnesioferrite in the first corona – an oxidation product from the pelletising plant – is reduced to magnetite, expelling magnesium to olivine and orthopyroxene. The result is referred to as the first olivine rim.
- In the same reduction step – from hematite to magnetite – the vitreous silica in the second corona will absorb various elements and form olivine, orthopyroxene and glass phases with varying composition.
- With further reduction of magnetite to wüstite in the pellets the first olivine rim will react with the second corona and a secondarily formed olivine phase appears, referred to as the second olivine rim. Elements in the previous second corona that does no fit the olivine lattice will remain as glass inclusions in the second olivine rim.
- In the lower shaft of the blast furnace where wüstite is trapped in the pellets core by a thick border of metallic iron the forsterite cores are consumed by the diffusion of magnesium and iron between olivine and wüstite. Forsterite cores survive in the metallic shell of pellets due to fast reduction of the wüstite phase.
- At the wall of the EBF in the lower shaft olivines are observed with a cracked glass rim. The cracks are a result of fast quenching as they are only observed in probed samples. The glass is potassium rich and is connected to the higher alkali deposition observed at the wall position in the EBF.
- The second olivine rim around forsterite cores that survive into the cohesive zone will be reduced to metallic iron, iron free olivine and silica. The silica attracts alkali and thus an alkali rich glass is formed furthering the reduction through deposition of alkali gas. Eventually the whole forsterite core will be reduced to these components.
- Quantitative studies with automated SEM technique confirm the manual SEM studies described above showing that the amount of olivine with a

composition more iron rich than the primary forsterite will form with increasing depth down to the lower shaft in the EBF.

- Studies on the effect of quench rate on pellets samples received from excavation versus probing show that there are quench products in the excavated pellets. These are the formation of magnetite in wüstite as wüstite grows out of its stability field with slow cooling. Further there is an increase in alkali deposition in the silicate phases due to condensation when quenching.
- Coating materials that were studied showed the formation of kalsilite on all samples, even on the uncoated reference sample. The use of coating for binding alkali is found unnecessary from a quality perspective.
- Mössbauer spectroscopy is shown to be a useful tool for the determination of the oxidation state of iron in pellets with increasing reduction.

11. Summary in Swedish

Mineralreaktioner och slaggbildning under reduktion av masugnspellets med olivintillsats

Sammanfattning

Det här arbetet fokuserar på mineralreaktionerna och slaggbildningen i LKABs järnmalmspellets med olivintillsats (MPBO) som utsatts för reducerande förhållanden i LKABs experimentsmasugn (EBF). Betoningen ligger på olivinets reaktioner med omgivande järnoxider. Flera faktorer influerar olivinets beteende. Studien genomfördes med mikro-analysmetoder; optisk mikroskopering, mikrosondanalys, mikro-Raman och Mössbauer spektroskopi och termodynamisk modellering. Under pelletstillverkningen, i oxiderande miljö vid höga temperaturer (1350°C), genomgår olivinet förändringar med slaggbildning och rimreaktioner med järnoxider och andra tillsatsmedel. För att kunna beskriva olivinets beteende i den komplexa masugnsprocessen med reducerande förhållanden måste man beakta faktorer som reaktionskinetik, reduktionsgrad av järnoxider, vertikala och horisontala positioner i masugnen och reaktioner med alkalier. Prover togs ut från EBF både genom sondning under drift och från utgrävning efter att EBF har stängts av och kylts ner.

Det ursprungliga slaggbildande olivinet består av forsterit – $(Mg_{1.9}Fe_{0.1})SiO_4$ – med inneslutningar av hematit och en amorf kiselrik fas, en första korona med lameller av magnesioferrit, olivin och ortopyroxen samt en andra korona bestående av amorft kvarts och magnesioferrit. Under reduktion i det övre schaktet i EBF (700-900°C) reduceras Fe^{3+} till Fe^{2+}. Den amorfa kvartsen i andra koronan tar upp alkalier, Al, Fe^{2+}, Mg och Ca och bildar glas med varierande sammansättning. Lamellerna i första koronan förenas i en enfasig rim med olivinsammansättning. Med ökande reduktion kommer glaset i den andra koronan att förenas med olivinrimmen och bildar en järnrik olivinrim och de grundämnen som inte passar in i olivinets kristallstruktur bildar inneslutningar inne i olivinrimmen. Diffusionen av magnesium och järn mellan olivin och järnoxiderna ökar med ökande temperatur i det nedre schaktet av EBF (750-1100°C). I den kohesiva zonen av EBF (1100-1200°C) är Fe^{2+} inte längre stabil och kommer att driva ut ur olivinet som metalliska järndroppar och olivinet bildar en komplex smälta

med den typiska sammansättningen; alkali-Al_2O_3-MgO-SiO_2. Alkalierna spelar en viktig roll i det sista steget där olivinkornet förtärs.

Kyltiden för prover tagna från sondningen och utgrävningen är minuter respektive timmar. En studie av kylhastighetens effekt på faser som uppträder i pellets visade inga stora skillnader i det övre schaktet. Men i det nedre schaktet separerar wüstit till wüstit och magnetit när wüstit växer ut sitt stabilitetsområde under långsam kylning av utgrävda prov. Det finns också en högre avsättning av alkalier och aluminium i glasfaserna som omger olivinerna i de utgrävda pellets vilket är ett resultat av att alkalie- och aluminiumgaser kondenserar på beskickningen i EBF under nedkylningen.

Beläggning på olivinpellets studerades i EBF med syftet att undersöka dess beteende, speciellt dess förmåga att ta upp alkalier. Beläggningsmaterialen bestod av kaolinit, bauxit, olivin och kalksten. Inga betydande reaktioner observeras i det övre schaktet. I det nedre schaktet var en majoritet av faserna amorfa och återspeglade originalsammansättningen hos beläggningsmaterialet. Avsättning av masugnsgas från EBF sker och kalsilit ($KAlSiO_4$) återfinns i alla prov; att använda beläggning för att binda alkalier är därför överflödigt ur den här kvalitativa studiens synpunkt.

Acknowledgements

I would like to express my deepest appreciation to my supervisor professor emiratus Hans Annersten for the dedication and encouragement you have shown during this thesis work. Thank you for introducing me to this field of research and thank you for all the helpful discussions and suggestions along the way.

My deepest gratitude also goes out to Dr Bo Lindblom for his help and kind support during the entire period of this work. Thank you for your patience with revising and giving constructive criticism of my manuscripts. Your encouragement of my work has helped me greatly.

I would also like to thank LKAB for financing my research on their products. I want to acknowledge Mats Hallin and Lawerence Hooey for providing me with the opportunity to perform this research. My gratitude also goes to LKAB's EBF research team in Luleå, it has been a great experience to work together with you. Thank you to the EBF workers who provided me with samples. I gratefully acknowledge Elin Rutqvist for helping me around with the instruments and lab work, but also for all the helpful discussions and suggestions. Thank you to Jenny Wikström for the encouragement and support with my manuscripts. I wish to say thank you to Harry Palo for providing great help in the sample preparation process, and thanks to CK-lab personell for sample preparation and chemical analyses.

I want to thank Hans Harryson for the great times spent in the microprobe lab. And thanks to the staff members and colleagues at the Department of Earth Sciences, Uppsala University for showing interest in my work and encouraging me. I would also like to thank the staff members and colleagues at the Division of Process Metallurgy, Luleå University of Technology for the encouragement and discussions.

I wish to thank my dear family for their support and sympathy during this time, especially to my husband Henrik Ryösä for his patience and always being there for me.

References

Biswas, A.K., (1981) Principles of blast furnace ironmaking. Cootha Publishing House, Brisbane.

Brämming, M., and Wikström, J-O. (2002) A blast furnace view on slags. *Scandinavian Journal of Metallurgy* 31, 88-99.

Chew, S.J., Zulli, P., Austin, P.R., Mathieson, J.G. and Yu, A.B. (2001) Assessment of the Blast Furnace Lower Zone Permeability Based on Liquids Flow Distribution. *Ironmaking Conference Proceedings*, ISS-AIME, USA, 60, pp. 241-52.

Chopelas, A., (1991). Single crystal Raman spectra of forsterite, fayalite, and monticellite. *American Mineralogist* 76, 1101-1109.

Darken, L.S. and Gurry, R.W. (1953) The physical chemistry of metals. McGraw-Hill, NY.

Davies, J., Moon, J.T. and Traice, F.B. (1978) Ironmaking Steelmaking 4, 151-161.

Garofalini, S.H. (1983) Behaviour of atoms at the surface of a $K_2O{\cdot}3SiO_2$ glass – a molecular dynamics simulation. Presented at the 85th Annual Meeting, The American Ceramic Society, Chicago, Illinois.

Geissberger, A.E, and Galeener, F.L. (1983) Raman studies of vitreous SiO_2 versus fictive temperature. *Physical Review B* 28, 6, 3266-3271.

Gasparov, L.V., Arenas, D., Choi, K-Y., Güntherodt, G., Berger, H., Forro, L., Margaritondo, G., Struzhkin, V.V., and Hemley, R., (2005). Magnetite: Raman study of the high-pressure and low-temperature effects. *Journal of Applied Physics* 97, 10A922-1-3.

Harrki, J., (1980). *On the hydrogen reduction of magnesiowüstite*. Report TKK-V-B 11-13, Helsinki University of Technology, Finland.

Hooey, L. (2004) *2nd International meeting on Ironmaking*, Vitória, Brazil, September 12-15, 803-815

Klein, C, 2002. *The 22nd Edition of the Manual of Mineral Science*, Johan Wiley & Sons, Inc.

Lin, C-C., (2003). Pressure-induced metastable phase transition in orthoenstatite ($MgSiO_3$) at room temperature: a Raman spectroscopic study. *Journal of Solid State Chemistry* 174, 403-411.

Lu, Y., Kong, L., and Lu, W-K. (1985) The effects of gangue minerals and fluxes on the quality of iron ore pellets. *ISS Transactions* 6, 1-13.

McMillan, P., Piriou, B., and Couty, R. (1984) A Raman study of pressure-densified vitreous silica. *The Journal of Chemical Physics* 81, 10:4234-4236.

McMillan, P.F., and Hofmeister, A. (1988) Infrared and Raman spectroscopy. *Reviews in Mineralogy and Geochemistry* 18, 1, 99-159.

Narita, K. (1978) On the permeability resistance of pellets containing MgO in the softening and melting zone of blast furnace. *Transactions ISIJ* 18, 712-720.

Niiniskorppi, V., (2004) Development of phases and structures during pelletizing of Kiruna magnetite ore. Doctoral thesis, Åbo Akademi University, Report 04-03

Roedder, E. (1952) A reconnaissance of liquidus relations in the system $K_2O{\cdot}2SiO_2$-FeO-SiO_2. *American Journal of Science*, Bowen volume, 435-448.

Shebanova, O.N., and Lazor, P., (2003). Raman spectroscopic study of magnetite ($FeFe_2O_4$): a new assignment for the vibrational spectrum. *Journal of Solid State Chemistry* 174, 424-430.

Shim, S-H., and Duffy, T.S., (2002). Raman spectroscopy of Fe_2O_3 to 62 GPa. *American Mineralogist* 87, 318-326.

Sterneland, J., and Jönsson, P.G. (2003) The use of coated pellets in optimising the blast furnce operation. *ISIJ International* 43, 26-35.

Wang, Z., Lazor, P., Saxena, S.K., and O'Neill, H. St. C., (2002). High pressure Raman spectroscopy of ferrite $MgFe_2O_4$. *Materials Research Bulletin* 37, 1589-1602.

Winell, S., Annersten, H., and Prakapenka, V., (2006). The high-pressure phase transformation and breakdown of $MgFe_2O_4$. *American Mineralogist* 91, 560-567.

Acta Universitatis Upsaliensis

Digital Comprehensive Summaries of Uppsala Dissertations from the Faculty of Science and Technology 575

Editor: The Dean of the Faculty of Science and Technology

A doctoral dissertation from the Faculty of Science and Technology, Uppsala University, is usually a summary of a number of papers. A few copies of the complete dissertation are kept at major Swedish research libraries, while the summary alone is distributed internationally through the series Digital Comprehensive Summaries of Uppsala Dissertations from the Faculty of Science and Technology. (Prior to January, 2005, the series was published under the title "Comprehensive Summaries of Uppsala Dissertations from the Faculty of Science and Technology".)

Distribution: publications.uu.se
urn:nbn:se:uu:diva-9389

ACTA
UNIVERSITATIS
UPSALIENSIS
UPPSALA
2008